

---

# Photoemission Electronic States of $(\text{Mn}_{1-x}\text{Fe}_x)_5\text{Si}_3$

B. PENC<sup>a</sup>, R. ZALECKI<sup>b</sup>, A. JEZIEFSKI<sup>c</sup>, A. SZYTUŁA<sup>a</sup>,  
A. KOŁODZIEJCZYK<sup>b</sup> AND V. IVANOV<sup>d</sup>

<sup>a</sup>M. Smoluchowski Institute of Physics, Jagiellonian University  
Reymonta 4, 30-059 Cracow, Poland

<sup>b</sup>Department of Solid State Physics, AGH University of Science and Technology  
Mickiewicza 30, 30-059 Cracow, Poland

<sup>c</sup>Institute of Molecular Physics, Polish Academy of Sciences  
Smoluchowskiego 17, 60-179 Poznań, Poland

<sup>d</sup>General Physics Institute, Russian Academy of Sciences  
Vavilov 38, 117-742 Moscow, Russia

(Received September 28, 2004; revised version April 4, 2005)

The core-level and valence band electronic states studies of single crystalline transition metal silicides  $(\text{Mn}_{1-x}\text{Fe}_x)_5\text{Si}_3$  ( $x = 0$  and  $0.05$ ) by the X-ray and ultraviolet photoemission spectroscopies are reported. The Mn  $2p$  core-level spectra for both compounds were ascribed to the relevant Mn sites in their crystal structure. The valence band spectra were compared with the result of *ab-initio* band calculations using the tight-binding linear muffin-tin orbital method. It was concluded that the enhancement of the spectral density within the 2 eV binding energy region below the Fermi energy comes from the effect of strongly correlated Mn  $3d$  electrons.

PACS numbers: 79.60.-i, 71.20.Gj, 71.15.Ap

## 1. Introduction

The isostructural intermetallic compounds  $\text{Mn}_5\text{Si}_3$  and  $\text{Fe}_5\text{Si}_3$  form continuous solid solutions in which the type of magnetic order varies as a function of temperature [1, 2].

Both investigated compounds crystallize in the hexagonal crystal structure type  $D8_8$ , space group  $P6_3/mcm$  (see Fig. 1). Manganese atoms are located in two different crystallographic sites:  $Mn_I$   $4d$  at  $\frac{1}{3}, \frac{2}{3}, 0; \frac{2}{3}, \frac{1}{3}, 0; \frac{1}{3}, \frac{2}{3}, \frac{1}{2}; \frac{2}{3}, \frac{1}{3}, \frac{1}{2}$ ; and  $Mn_{II}$   $6g$  at  $x, 0, \frac{1}{4}; 0, x, \frac{1}{4}; \bar{x}, \bar{x}, \frac{1}{4}; \bar{x}, 0, \frac{3}{4}; 0, \bar{x}, \frac{3}{4}; x, x, \frac{3}{4}$ . The Si atoms occupy also  $6g$  site with the different values of the  $x$  parameter. The value of the  $x$  parameter are equal to 0.2358(6) and 0.5992(15) for Mn and Si, respectively. The atomic surroundings of Mn atoms at the different crystallographic positions are presented in Fig. 1. The Mn atoms in  $4d$  site have 14 neighbours (2  $Mn_I$ , 6  $Mn_{II}$ , 6 Si) while in  $6g$  — 15 neighbours (4  $Mn_I$ , 6  $Mn_{II}$ , 5 Si). The interatomic distances are given below in Å:

$Mn_I - 2 Mn_I$ :	2.41	$Mn_{II} - 4 Mn_I$ :	2.96
$Mn_I - 6 Mn_{II}$ :	2.96	$Mn_{II} - 6 Mn_{II}$ :	2.82(2×) and 2.91(4×)
$Mn_I - 6 Si$ :	2.43	$Mn_{II} - 5 Si$ :	2.41(2×), 2.51, and 2.66(2×)

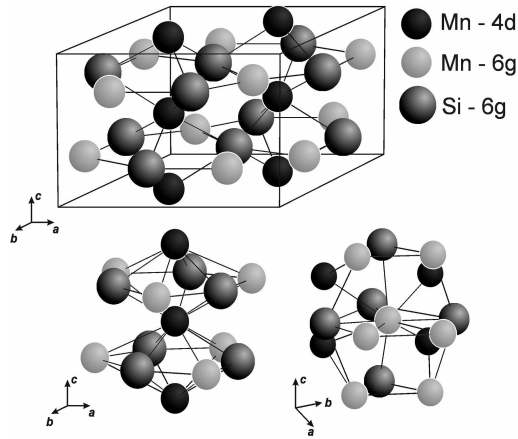


Fig. 1. Crystal structure of  $Mn_5Si_3$  and atom coordination polyhedra  $Mn_I$  and  $Mn_{II}$  (see the text).

The parent compound  $Mn_5Si_3$  shows a Curie–Weiss paramagnetic state above the Néel temperature 99 K and an additional first-order transition at 66 K. Below this temperature it exhibits a non-collinear complex antiferromagnetic structure [3]. The  $Fe_5Si_3$  compound is ferromagnetic below 376 K [2]. From neutron diffraction [1] and Mössbauer effect [4] it was deduced that Mn and Fe atoms preferentially occupy the  $6(g)$  and  $4(d)$  positions, respectively. The temperature dependence of resistivity along the  $a$  axis as well as along  $c$  axis in zero magnetic field and at 12 T was measured for  $Mn_5Si_3$  in the paper [5] showing a metallic conductivity and a strong effect of the complex magnetic behaviour below the Néel temperature.

To our knowledge only one paper [6] was published on electron photoemission studies for a single crystalline compound  $\text{Mn}_5\text{Si}_3$ . The sample came from the same source as our samples. The authors performed the photoemission experiments using synchrotron radiation at 900 eV with the energy resolution of about 100 meV for the valence band spectra and of about 200 meV for the Mn  $3s$ ,  $2p$ ,  $3p$ ,  $3d$  and Si  $3s$ ,  $3p$  core-level spectra. Among others, they concluded that the valence band spectrum close to the Fermi energy consists mostly of the Mn  $3d$  electron states and corresponds well to the density of states (DOS) calculated in the paper [7]. For the low temperature magnetic state it was suggested that some Mn sites are providing itinerant electrons and some more localized moments [8]. However, the nature of electronic states is still unclear and the effect of iron substitution is unknown.

This paper reports results of X-ray and ultraviolet electron photoemission measurements (XPS/UPS) for  $\text{Mn}_5\text{Si}_3$  and  $(\text{Mn}_{0.95}\text{Fe}_{0.05})_5\text{Si}_3$  single crystals. The data concerning the valence band spectra are compared with *ab-initio* electronic band structure calculations using the tight-binding linear muffin-tin orbital (TBLMTO) approach [9]. On the basis of the results the electronic structure of the compounds was determined.

## 2. Experimental

Two single crystals  $\text{Mn}_5\text{Si}_3$  and  $(\text{Mn}_{0.95}\text{Fe}_{0.05})_5\text{Si}_3$  were prepared by the Czochralski method in a helium atmosphere using a beryllium oxide crucible [5].

The *dc* magnetic susceptibility of  $\text{Mn}_5\text{Si}_3$  as a function of temperature was measured in our previous paper [1] and in the paper [10] showing the Néel temperature  $T_N \cong 70$  K. In the present paper the real component of *ac* magnetic susceptibility of  $(\text{Mn}_{0.95}\text{Fe}_{0.05})_5\text{Si}_3$  as a function of temperature was measured by the standard mutual inductance bridge in the zero field cooling procedure (ZFC) at 189 Hz. The *ac* magnetic field of rms amplitude of 0.1 Oe was applied in the *ab*-plane of the sample.

The XPS spectra were measured at room temperature using the Leybold LHS10 electron photoemission spectrometer with Mg  $K_\alpha$  ( $h\nu = 1253.6$  eV) radiation. The total energy resolution of the spectrometer with a hemispherical energy analyzer was about 0.75 eV for Ag  $3d$  line. Binding energies are referred to the Fermi level ( $E_F = 0$ ). The spectrometer was calibrated using the Cu  $2p_{3/2}$  (932.5 eV), Ag  $3d_{5/2}$  (368.1 eV), and Au  $4f_{7/2}$  (84.0 eV) core-level photoemission spectra. Measurements were carried out at room temperature. Surfaces of the compounds were mechanically cleaned by scraping with a diamond file in a preparation chamber under high vacuum ( $10^{-9}$  mbar) and then immediately moved into the analysis chamber. This procedure was repeated until the C  $1s$  and O  $1s$  core-level peaks were negligibly small or did not change after further scraping. Such a procedure of cleaning was performed before each XPS measurement. The Shirley method [11] was used to subtract the background and so prepared experi-

mental spectra were numerically fitted using the proper mixture of the Gaussian and Lorentzian curves.

The UPS spectra were collected in room temperature with an Omicron spectrometer equipped with the ARUPS 65 energy analyzer and with a high intensity ultraviolet He I source of photon energy of 21.2 eV. The energy resolution of the spectrometer calibrated for the Fermi edge of Ag was about 70 meV. A surface of the specimen was scraped prior to measurements and then cleaned by heating up to 520°C and annealing *in situ* in ultra high vacuum conditions. The Taugard [12] procedure was used to subtract the secondary electron background.

### 3. The method of calculation

The electronic structure was calculated by *ab-initio* self-consistent TBLMTO method [9] within the framework of the local spin density (LSD) approximation. The scalar-relativistic approximation for band electrons and the fully-relativistic treatment of the frozen core electrons were used. The exchange correlation potential was assumed in the form of von Barth and Hedin [13] with gradient corrections [14]. The self-consistent calculations were performed in the atomic sphere approximation (ASA) for the experimental values of the lattice parameters. The values of the atomic sphere radii were chosen in such a way that the sum of all atomic sphere volumes was equal to the volume of the unit cell. In the band calculations the initial atomic configurations were assumed according to the periodic table of elements.

### 4. Results and their analysis

The temperature dependence of *ac* susceptibility for  $(\text{Mn}_{0.95}\text{Fe}_{0.05})_5\text{Si}_3$  is shown in Fig. 2.

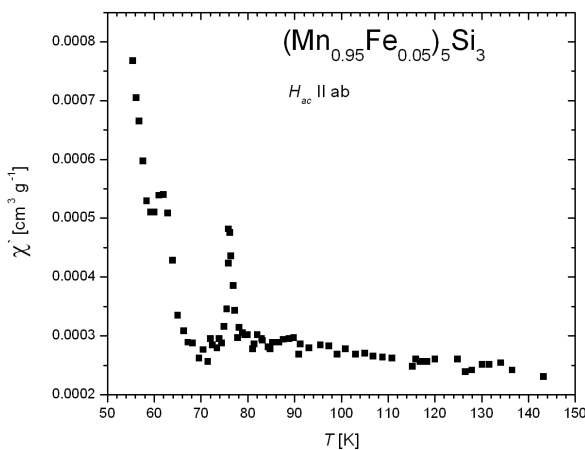


Fig. 2. Temperature dependence of *ac* susceptibility of  $(\text{Mn}_{0.95}\text{Fe}_{0.05})_5\text{Si}_3$ .

The Néel temperature is 76 K and the first-order transition is at  $T_t = 62$  K as compared to 70 K and 66 K for  $\text{Mn}_5\text{Si}_3$ , respectively [10].

Figure 3 shows the XPS spectra of the  $\text{Mn}_5\text{Si}_3$  and  $(\text{Mn}_{0.95}\text{Fe}_{0.05})_5\text{Si}_3$  compounds in a wide binding energy range of 0–1000 eV (Fig. 3a) and in the vicinity of the Mn  $2p$  core-level spectrum and the Auger lines: Mn  $L_3M_{23}M_{45}$  and Mn  $L_3M_{45}M_{45}$  (Fig. 3b). Binding energies are related to the Fermi level ( $E_F = 0$  eV). A small contamination of oxygen at about binding energy 530 eV (O  $1s$  line) and of carbon at about 290 eV (C  $1s$  line) is visible (see Fig. 3a).

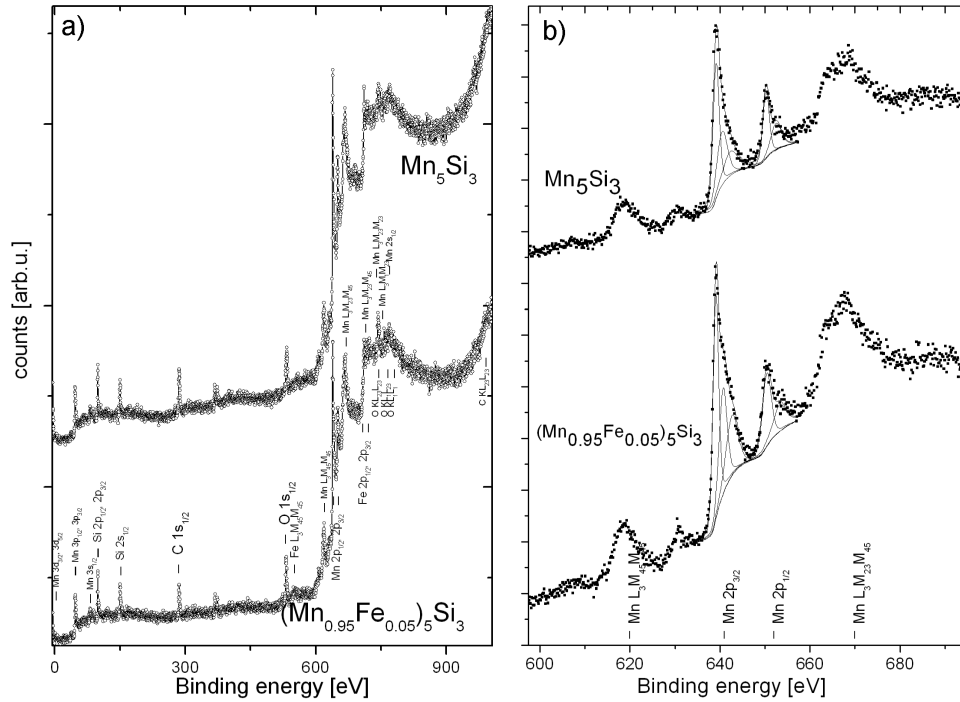


Fig. 3. XPS Mg  $K_\alpha$  spectra of  $\text{Mn}_5\text{Si}_3$  and  $(\text{Mn}_{0.95}\text{Fe}_{0.05})_5\text{Si}_3$  compounds with the indicated core-level lines (a), Mn  $2p$  core-level photoemission spectra of  $\text{Mn}_5\text{Si}_3$  and  $(\text{Mn}_{0.95}\text{Fe}_{0.05})_5\text{Si}_3$  (b). Solid curves are the results of fittings.

The Mn  $2p$  core-level spectrum in Fig. 3b shows the splitting due to the spin-orbit interaction. The peaks at  $E_B \cong 640$  eV and 650 eV correspond to the energy difference between  $2p_{3/2}$  and  $2p_{1/2}$  states. The both peaks are composed of weaker peak at higher binding energy ( $E_B$ ) and a stronger peak at lower  $E_B$ . Therefore, both peaks have been deconvoluted into two components corresponding to the positions of the Mn atoms in a crystal unit cell. The intensity ratio of the Mn(1) to Mn(2) is roughly 2:3 for both compounds. The Table collects the determined values of the binding energy and values of the spin-orbit splitting  $\Delta E$  for Mn  $2p_{3/2}$ , Mn  $2p_{1/2}$ , and pure metallic Mn  $2p$  levels [14, 15].

TABLE

The binding energy  $E_B$  of Mn  $2p_{3/2}$  and  $2p_{1/2}$  levels and the spin-orbit splitting  $\Delta E$  for  $\text{Mn}_5\text{Si}_3$ ,  $(\text{Mn}_{0.95}\text{Fe}_{0.05})_5\text{Si}_3$  and pure metallic Mn.

Compound		$E_B$ [eV]		$\Delta E$ [eV]
		$2p_{3/2}$	$2p_{1/2}$	
$\text{Mn}_5\text{Si}_3$	6g site	639.1	650.2	11.1
	4d site	640.4	652.5	12.1
$(\text{Mn}_{0.95}\text{Fe}_{0.05})_5\text{Si}_3$	6g site	639.1	650.4	11.3
	4d site	640.7	653.2	12.5
Mn [14]		638.7	650.0	11.3

The difference between Mn sites is consistent with the crystal structure data. The Mn atoms occupy two different crystallographic sites: 6g and 4d (see Fig. 1). The corresponding values of the binding energy of the Mn atoms at 6g site are close to the value of pure metallic Mn while for those at 4d site the significantly bigger chemical shift than for Mn was detected. For  $(\text{Mn}_{0.95}\text{Fe}_{0.05})_3\text{Si}_5$  the values for 6g site are the same as for  $\text{Mn}_5\text{Si}_3$  while for 4d site the increase in the binding

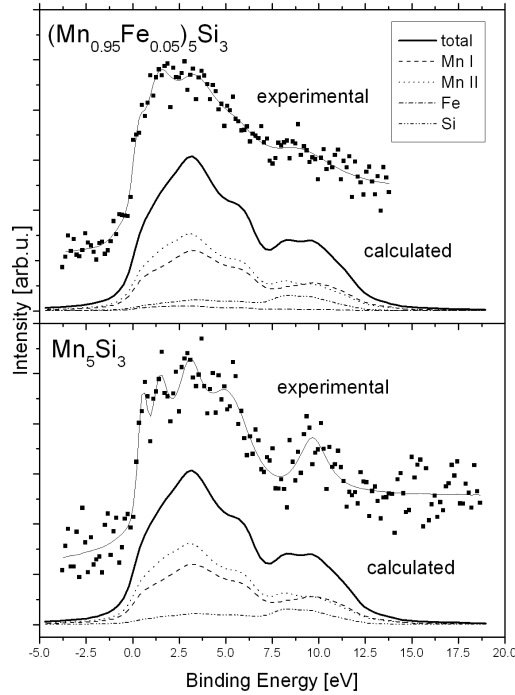


Fig. 4. Comparison of the XPS valence band of  $\text{Mn}_5\text{Si}_3$  and  $(\text{Mn}_{0.95}\text{Fe}_{0.05})_3\text{Si}_5$  with the calculated DOS (Fig. 5) which were convoluted by Lorentzian curves of the half-width 0.75 eV. The total and partially DOS from  $\text{Mn}_{\text{I}}$ ,  $\text{Mn}_{\text{II}}$ , Fe, and Si atoms are indicated.

energy and spin-orbit splitting has been observed. This result indicates that the doping Fe atoms to the 4d sites affects the electronic state of Mn atoms in other 4d sites.

The XPS valence bands (VB) of both investigated compounds are presented in Fig. 4.

The bands extend from the Fermi energy at  $E = 0$ , to the binding energy of about 12.5 eV. The spectra were numerically fitted using five lines each consisting of a proper mixture of the Gaussian- and Lorentzian-shaped lines (the solid curves in Fig. 4).

Figure 5 shows the calculated partial (Mn, Fe, and Si) and the total DOS for  $Mn_5Si_3$  and  $(Mn_{0.95}Fe_{0.05})_5Si_3$ . In Fig. 4 the calculated density of states convo-

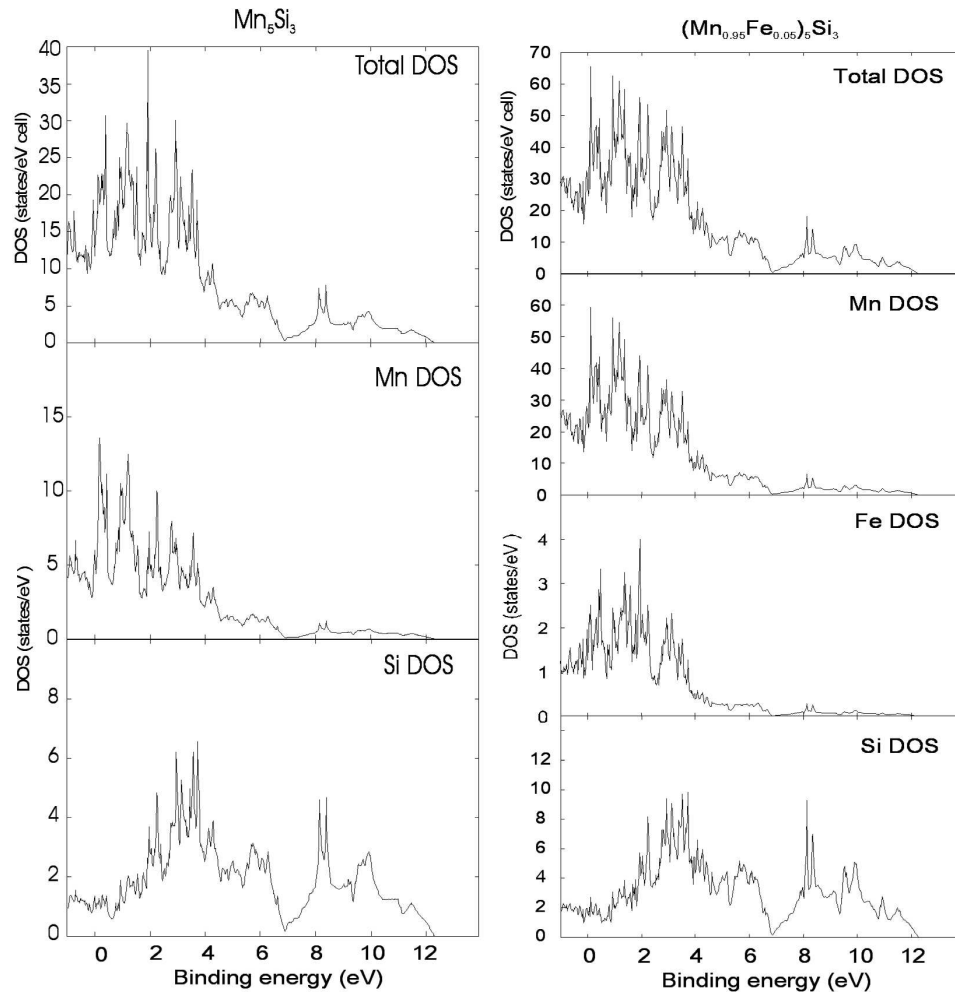


Fig. 5. The calculated partial (Mn, Fe, Si) and total density of states of paramagnetic  $Mn_5Si_3$  and  $(Mn_{0.95}Fe_{0.05})_5Si_3$  compounds.

luted by Lorentzian curves of the half-width 0.75 eV due to the energy resolution of the spectrometer were compared with the recorded spectra.

As can be seen from Fig. 5 the Mn partial density of states gives the five maxima between 0 and 5 eV at 0.2, 1.0, 2.15, 2.8, and 3.5 eV. The Si 3s electrons give a few times smaller spectral intensity at 3.4 and 5.9 eV and the Si 3p electrons at 8.4 and 9.9 eV than the spectral intensity from Mn 3d electrons. The total density of states for  $(\text{Mn}_{0.95}\text{Fe}_{0.05})_5\text{Si}_3$  is similar to those calculated for  $\text{Mn}_5\text{Si}_3$ . The Fe 3d states form a broad but much less intense maximum in the region between  $E_F$  and 4 eV which coincides with the Mn 3d states. On the basis of the calculations one can conclude that the maxima at about 0.6, 1.5, 3.0, and 5.0 eV in the experimental spectrum of  $\text{Mn}_5\text{Si}_3$  are connected with the Mn 3d states and the photoemission peak at about 9.7 eV comes from the electrons of the Si 3p state.

In the spectrum of  $(\text{Mn}_{0.95}\text{Fe}_{0.05})_3\text{Si}_3$  the small shifts of the binding energies of those maxima have been detected and are equal to 0.55, 1.55, and 3.3 eV for Mn 3d state and 8.5 eV for Si 3p state. In general, the valence band photoemission spectra of both compounds agree qualitatively with the result of the band calculations.

The UPS spectra were recorded using the ARUPS electron energy analyzer with the energy resolution of about 70 meV to look at more details on the valence bands in the vicinity of the Fermi energy. In Fig. 6 the UPS spectra for both compounds at room temperature are shown in the 2 eV region below the Fermi edge.

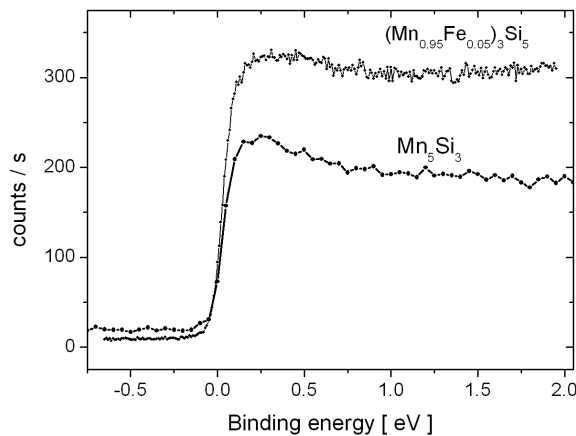


Fig. 6. The UPS valence band spectra at room temperature.

The two most important observations from the UPS spectra are: (1) the very sharp Fermi edge and (2) the enhancement of electronic states just below  $E_F = 0$  within 2 eV binding energy interval  $E_B$  (see Fig. 6). From the comparison with

our calculations (see Fig. 5) as well as the literature band structure ones for the parent compound  $Mn_5Si_3$  [7] the enhancement comes entirely from  $3d$  Mn states whereas the Si  $3p$  states contribute to the bottom of the band. The enhancement reveals the effect of strongly correlated  $3d$  electrons on electronic properties of the compounds.

## 5. Conclusions

We have performed measurements of core-level and valence band photoemission states of two single crystals  $Mn_5Si_3$  and  $(Mn_{0.95}Fe_{0.05})_5Si_3$  using XPS/UPS methods with conventional photon sources. The core-level spectra were found to consist of two components connected with two crystallographic sites of Mn ions. The substitution of Fe atoms to the  $4d$  site affects electronic state of Mn atoms in this site and the chemical shift is significantly bigger. The valence band photoemission spectra of both compounds are very similar and agree qualitatively with the paper [6] as well as with our TBLMTO and published in [7] band structure calculations. On this basis we concluded that the enhancement of  $3d$  Mn electronic states just below the sharp Fermi energy (see Fig. 6) gives rise to an effect of strongly correlated  $3d$  electrons on the electronic and magnetic properties of the compounds.

## Acknowledgments

This work was financially supported by the Physics Institute of the Jagiellonian University and by Faculties of Physics and Applied Computer Science, AGH University of Science and Technology, Cracow.

## References

- [1] H. Bińczycka, Ž. Dimitrijevic, B. Gajić, A. Szytuła, *Phys. Status Solidi A* **19**, K13 (1973).
- [2] R. Hang, G. Kappel, A. Jaegle, *J. Phys. Chem. Solids* **41**, 539 (1980).
- [3] P.J. Brown, J.B. Forsyth, V. Nunez, F. Tasset, *J. Phys., Condens Matter* **4**, 10025 (1992).
- [4] V. Johnson, J.F. Weiher, C.G. Fredrick, D.B. Rpgers, *J. Solid State Chem.* **4**, 311 (1972).
- [5] L.I. Vinokurova, V.J. Ivanov, E.T. Kulatov, *Trudy Instituta Obshchej Fiziki Akademii Nauk SSSR* **32**, 67 (1999).
- [6] A. Irizawa, A. Yamasaki, M. Okazaki, S. Kasai, A. Sekiyama, S. Imada, S. Suga, E. Kulatov, H. Ohta, T. Nanba, *Arxiv: cond-mat/0209654* v1 28 Sep 2002.
- [7] L. Vinokurova, V. Ivanov, E. Kulatov, A. Vlasov, *J. Magn. Magn. Mater.* **90-91**, 121 (1990).

- [8] A.Z. Menshikov, A.M. Balagurov, A.I. Beskrovney, A.P. Vokhmyanin, D.M. Morozov, *Mater. Sci. Forum* **321-324**, 659 (2000).
- [9] O.K. Anderson, O. Jepsen, *Phys. Rev. Lett.* **53**, 2571 (1984).
- [10] R.P. Krentsis, I.Z. Radovski, P.V. Gel'd, L.P. Andreeva, *Zh. Neorg. Khim.* **10**, 2192 (1965).
- [11] D.A. Shirley, *Phys. Rev. B* **5**, 4709 (1972).
- [12] S. Taugard, *Surf. Sci.* **216**, 343 (1989).
- [13] U. von Barth, L. Hedin, *J. Phys. C* **5**, 1629 (1972).
- [14] D. Hu, D.C. Langreth, *Phys. Scr.* **32**, 391 (1985).
- [15] S. Hüffner, *Photoemission Spectroscopy*, Springer Verlag, Berlin 1994, p. 453.